MECHANISMS OF SIGNAL TRANSDUCTION:

Reversible and Specific Extracellular Antagonism of Receptor-Histidine Kinase Signaling

Gholson J. Lyon, Jesse S. Wright, Arthur Christopoulos, Richard P. Novick and Tom W. Muir

Reversible and Specific Extracellular Antagonism of Receptor-Histidine Kinase Signaling*

Gholson J. Lyon‡§§, Jesse S. Wright§, Arthur Christopoulos¶‖, Richard P. Novick§, and Tom W. Muir‡ ‡‡**

From the ‡Laboratory of Synthetic Protein Chemistry, The Rockefeller University, New York, New York 10021, the §Molecular Pathogenesis Program, Skirball Institute of Biomolecular Medicine, New York University Medical Center, New York, New York 10016, and the ¶Department of Pharmacology, University of Melbourne, Parkville, Victoria 3010, Australia

Staphylococcal pathogenesis is regulated by a two-component quorum-sensing system, *agr*, activated by a self-coded autoinducing peptide (AIP). The *agr* system is widely divergent and is unique in that variant AIPs cross-inhibit *agr* activation in heterologous combinations. Cross-inhibition, but not self-activation, is widely tolerant of structural diversity in the AIPs so that these two processes must involve different mechanisms of interaction with the respective receptors. Herein, we have utilized this naturally occurring antagonism to demonstrate that both activation and inhibition are reversible and that activators and inhibitors interact at a common site on the receptor. These results suggest that molecules designed to compete with natural agonists for binding at receptor-histidine kinase sensor domains could represent a general approach to the inhibition of receptor-histidine kinase signaling.

Receptor-histidine kinases (RHKs)[1] have been extensively characterized in bacteria and are present in archaea, microbial eukarya, and higher plants, where they have recently been shown (in *Arabidopsis)* to play a role in hormone signaling (1). In bacteria, RHKs are involved in sensing the environmental surroundings. Many of these kinases contain two transmembrane helices flanking a periplasmic domain. This domain contains the binding site for the appropriate ligand, such as metal ions (Mg^{2+} in the case of PhoP) (2). Many RHKs have been shown to exist as preformed dimers in the inner cell membrane of Gram-negative bacteria (3). In the case of EnvZ, a pair of cytoplasmic α-helices from each monomer form a four-helix bundle (4). In Gram-positive bacteria, pheromone-inducible RHKs usually have a polytopic sensor domain, containing 5–8 membrane-spanning segments. RHKs predicted to possess this polytopic sensor domain include AgrC from *Staphylococcus aureus* (5), ComD from *Streptococcus pneumoniae* (6), ComP from *Bacillus subtilis* (7), and SapK from *Lactobacillus sakei* Lb706 (8). These RHKs respond to secreted signaling peptides, which bind to the sensor domain to initiate the transmembrane signal that activates the intracellular histidine kinase (HK). Notably, there is at least one RHK in *Escherichia coli*, UhpB, which contains 6–8 transmembrane helices and which is also thought to function as a homodimeric complex (9).

The *agr* system in *S. aureus* is the most fully characterized in terms of the receptor-ligand interaction. Density-dependent accumulation of an extracellular peptide, known as the AIP and derived from processing of the prepeptide, AgrD, triggers activation of the receptor-histidine kinase, AgrC. This leads to a downstream virulence response via the unique regulator, RNAIII (10). This signaling process is one example of density-dependent or "quorum-sensing" systems widespread in bacteria (11, 12). The sequence of the AIPs is highly variable, resulting in at least four specificity groups within *S. aureus* and many others in other staphylococcal species (13–15). All strains within a group produce the same AIP. The *agrB*, -*D*, and -*C* region varies in concert so as to maintain the specificity of AIP processing and function (15). Remarkably, each AIP has two biological functions; it can activate the virulence response within its own specificity group and inhibit the virulence response in other groups (15). This is a form of bacterial competition that does not result in growth inhibition but rather in virulence attenuation, presumably resulting in an advantage for the strain producing the most abundant and/or most potent AIP. Note that in lactobacilli, pneumococci, and bacilli, although there are many natural signaling peptide variants, in no case has cross-inhibition been reported. Thus, *agr* is the only bacterial two-component system in which natural antagonists have been identified so far.

Extensive structure-activity relationship studies have been performed on the AIPs (16, 17) and have shown that (i) the AIPs contain a thiolactone structure that is absolutely required for potent biological activity; (ii) this linkage is formed from the condensation of the α-carboxyl group of the peptide with the sulfhydryl group of a conserved cysteine, which is always the fifth amino acid from the C terminus (see Fig. 1); (iii) the lactam and lactone analogs of AIP-II are potent *agr* cross-group inhibitors but lack activity against self, at concentrations up to 5 μM (16); (iv) the N-terminal four amino acids of the group II AIP, collectively referred to as the "tail region," are necessary for self-

[1] The abbreviations used are: RHK, receptor-histidine kinase; HK, histidine kinase; AIP, autoinducing peptide; V_{init}, initial velocity of cleavage of nitrocefin by β-lactamase assay; EC_{50}, half-maximal effective concentration.

activation but not for cross-group inhibition (16); and (v) a truncated version of AIP-II, lacking the tail region but retaining the thioester bond (see Fig. 1), is a global *agr* inhibitor (18). In this report, the AIPs are identified as AIP-X, where X represents the specificity group from which the AIP is derived. For example, the group I AIP is referred to as AIP-I, and the truncated group II AIP is referred to as trAIP-II.

It has been demonstrated that the N-terminal region of AgrC, the sensor domain, contains the agonist AIP binding site (5). Sequence and PhoA fusion analyses suggest that the sensor domain is composed of five or six transmembrane helices, depending on whether the N terminus of the protein is placed on the inside or outside of the cell (5). More recently, it has been shown that AgrC and the AIP are the only group-specific components of the system that are required for *agr* activation and inhibition (18). In the present study, we have demonstrated unequivocally that the sensor domain of AgrC confers group-specific activation and inhibition by the AIPs, and we have begun to investigate ligand binding with special reference to the mechanism of antagonism. We have previously speculated that the acylating nature of the thioester bond might play some role in activation of the receptor (16). In this report, it is shown that the AIP-receptor interaction is reversible, ruling out a stable covalent bond between ligand and receptor. Agonists and antagonists most likely interact via a common site at the sensor domain of AgrC.

EXPERIMENTAL PROCEDURES

Bacterial Strains and Growth Conditions—The bacterial strains used have been described in a previous study (18). These strains are RN9222 (CA1-I), RN9372 (CA2-II), and RN9367 (CA2-I). All reconstituted strains are provided with a descriptor in the format CAx-y, which indicates group x *agrC* and *agrA* on the group y *agr*-null background, and are referred to under "Results" as group I or group II based on the group-specific *agrC* being expressed. *S. aureus* cells were grown in CYGP broth (19) with shaking at 37 °C. Overnight cultures on GL plates (19) were routinely used as inocula. Cell growth was monitored with a Klett-Summerson colorimeter with a green (540-nm) filter (Klett, Long Island City, NY). Antibiotics used were erythromycin (10 μg/ml) and tetracycline (5 μg/ml).

Synthetic Peptides—All AIP peptides were chemically synthesized and purified as described (16) and were characterized as >95% pure using high pressure liquid chromatography, mass spectrometry, and two-dimensional ^{1}H NMR. The concentrations of stock solutions were calculated based on UV absorbance measurements, utilizing extinction coefficients determined by amino acid analysis.

Agr Activation and Inhibition Assays—Assays were performed with bacterial cultures in early exponential phase ($\sim 2 \times 10^8$ cells/ml). Synthetic peptides in 25% propylene glycol, 0.05 M phosphate, pH 5.7, were added at various concentrations to 96-well plates, and cultures were incubated in duplicate with shaking at 37 °C for 60 or 90 min in a THERMOmax microplate reader (Molecular Devices) with monitoring of cell density at A_{650}, followed by determination of *agr* activation by the β-lactamase/nitrocefin assay (20).

Chimeric Receptor Construction—Chimeric receptors were assembled by fusing the N-terminal sensor domain of the group I and group II *agrC* coding sequence to the group IV *agrC* HK-*agrA* coding region in the reporter construct pRN7107 (18). The QuikChange mutagenesis kit (Stratagene) was used to introduce an *Afl*II restriction site at the probable junction between the (N-terminal) sensor and (C-terminal) HK domains in *agrC* (JSW1 and JSW2), creating pRN7107-2. The group I and group II sensor domains were amplified from pRN7062 and pRN7105 (18) with *Pwo* polymerase (Roche Molecular Biochemicals) using a common upstream primer (JSW5) and downstream primers complementary to either group I (JSW2) or group II (JSW7) incorporating the new *Afl*II site. The PCR products were digested with *Pst*I and *Afl*II and ligated into pRN7107-2 digested with the same enzymes to create the chimeric reporters pRN7107-2-GI and pRN7107-2-G2 (referred to as group I chimera and group II chimera). Plasmid inserts were identified by restriction analysis and DNA sequencing.

Primer sequences (complementary primers) were as follows: JSW1, 5′-CAATTTCTCC**CTTAAG**GAGATGAAATA-3′; JSW2, 5′-TATTTC-ATCTCC**CTTAAG**GAGAAATTG-3′; upstream primer, JSW5 (5′-GCA-

CATGGTGCACATGCACCT-3′); downstream primers, JSW2 (for group I) and JSW7 (5′-TATTTCATCTCC**CTTAAG**GGTGAAAAG-3′) (for group II).

Plasmid DNA from the corresponding *E. coli* DH5α derivative was introduced into the restriction-defective *S. aureus* strain, RN4220, by the protoplast method (19). Plasmids were then moved into the group I *agr*-null cell line, RN6911, by phage transduction (19).

Functional Binding and Competition Experiments—RN9222 (CA1-I) cells or RN9372 (CA2-II) cells (both at 9×10^8 cells/ml) were treated for 1 h with AIP-I or -II at 1 μM. Aliquots (1 ml) of the cells were pelleted and resuspended in 1 ml of CYGP broth. This washing procedure was repeated up to 10 times. After the washes, cells were resuspended in CYGP broth with or without AIP-I or -II at a concentration of 1 μM. In one set of experiments, trAIP-II was added at 1.0 or 3.3 μM. Time points were then taken to monitor the kinetics of β-lactamase induction. Washing exerted only a minimal effect on subsequent growth, and the data were normalized to cell density to account for any small differences. Control experiments in which activated cells were either untreated or reactivated with their group-specific AIPs after washing showed that washing had a minimal effect on subsequent activation. All experiments were performed at least twice, and the data were combined.

Effects of Antagonist AIP Preincubation and Washing on Subsequent Activation—In the case of cross-group inhibition, 3 ml of RN9222 (CA1-I) cells (9×10^8 cells/ml) were preincubated for 1 h (or 5 min) with either AIP-II at 1 μM or 25% propylene glycol, 0.05 M phosphate (pH 5.7) buffer. Time point zero was then taken with 50 μl of cells added to 75 μl of CYGP supplemented with sodium azide at 5 mM, and the samples were placed on ice. Cultures were then divided into 500-μl aliquots, pelleted, washed with 1 ml of CYGP broth, pelleted again, and then resuspended in 495 μl of CYGP broth with the addition of either buffer alone or AIP-I at 1 μM. Cells were then incubated with shaking at 37 °C, and samples were taken every 30 min as described above. The β-lactamase assay was performed at the conclusion of 210 min, and the data were normalized by calculating the induction ratio (induced/basal) at each time point. Data are quoted ± S.E., and are derived from several time points (150, 180, and 210 min) combined after normalization.

In the case of self-inhibition, 1 ml of RN9372 (CA2-II) cells were preincubated with or without trAIP-II at 1 μM for 30 min at 37 °C. The cells were pelleted, washed, pelleted again, and resuspended in 1 ml of CYGP broth. The cells were then treated for 60 min with AIP-II at varying concentrations, and *agr* activation was evaluated by the nitrocefin assay. The data were used to plot concentration-response curves, from which EC_{50} values were derived. These values are quoted ± S.E.

Order of Addition Experiments—RN9222 (CA1-I) cells (80 μl at 9×10^8 cells/ml) were treated in duplicate with varying [AIP-II]. AIP-I was added at 100 nM, either 5 min before, simultaneously, or 5 min after the addition of the antagonist. The cells were incubated at 37 °C in a 96-well plate with shaking during these 5-min periods. The cells were then incubated for 60 min at 37 °C. *Agr* activation was evaluated by the β-lactamase assay as above. A similar series of experiments was performed on RN9372 (CA2-II) cells using AIP-II *versus* trAIP-II. Data were collected as β-lactamase activity (V_{init} in mOD/min) and then normalized to percentage of maximal activation. Data are ± S.E.

Agonist-Antagonist Interactions: Concentration-Response Curves—For the activation experiments, 80 μl of cells (9×10^8 cells/ml) were treated in duplicate with AIP agonist at varying concentrations in the absence or presence of the antagonist at fixed concentrations up to 1000 nM. Incubation was for 1 h at 37 °C, and *agr* activation was evaluated by the β-lactamase assay.

For inhibition experiments, 80 μl of cells (9×10^8 cells/ml) were treated in duplicate with the antagonist in the presence of a fixed concentration of the agonist at concentrations up to 1000 nM. Incubation was for 1 h at 37 °C, followed by the β-lactamase assay.

Studies with Asparagine to Alanine Modified AIP-II (N3A)—For self-inhibition experiments, RN9372 (CA2-II) cells (at 9×10^8 cells/ml) were incubated in duplicate in a 96-well plate with AIP-II at 100 nM and varying concentrations of the N3A AIP-II analog or of other alanine-modified AIP-II analogs (16) for 60 min at 37 °C. *agr* activation was evaluated by the nitrocefin assay, and the data were used to plot concentration-response curves. *agr* activation of RN9372 (CA2-II) cells and cross-group inhibition experiments utilizing cell line RN9222 (CA1-I) with the alanine-scanned AIP-II analogs were performed as described (18).

Studies with AIP-II Lactam Analog—RN9372 (CA2-II) cells or RN9367 (CA2-I) cells (both at 9×10^8 cells/ml) were incubated for 60 min at 37 °C in duplicate in a 96-well plate, with varying [AIP-II lactam]. *Agr* activation was evaluated by the nitrocefin assay, and the data were used to plot concentration-response curves. The effect of
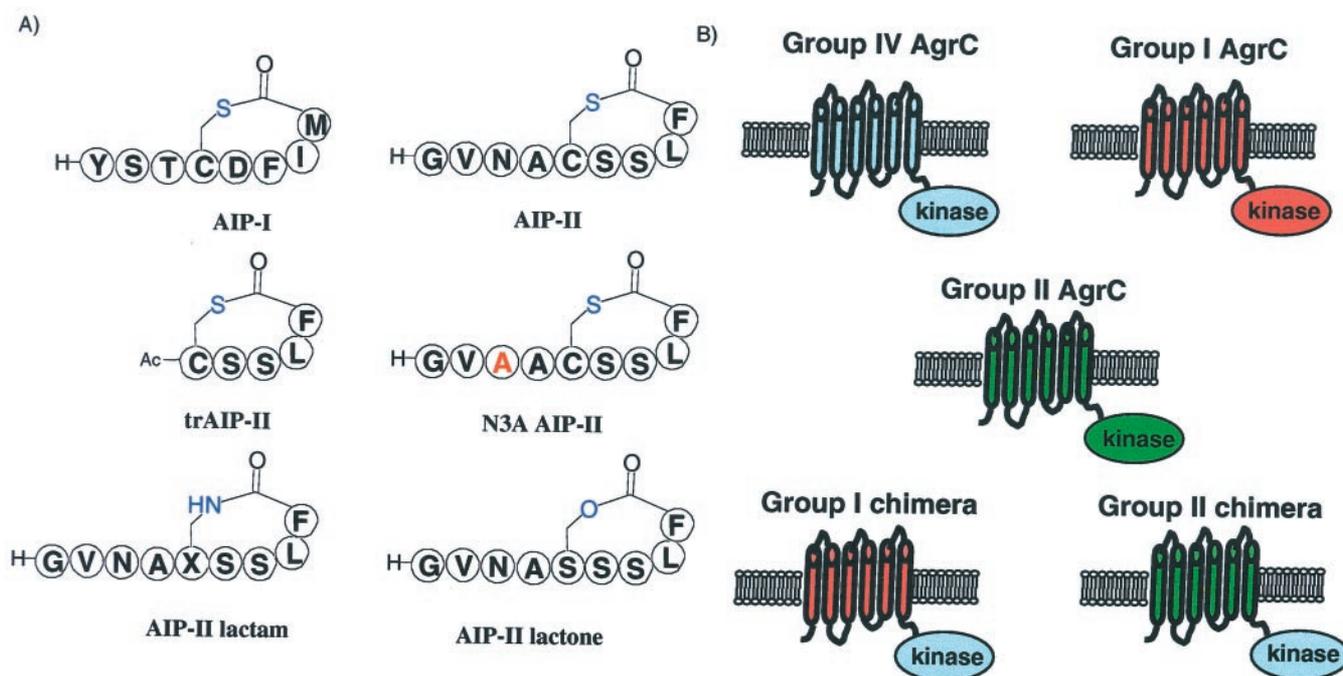
FIG. 1. **Structures of AIPs and AgrC RHKs.** *A*, structures of the AIPs used in this study. Single-letter amino acid codes are depicted in the *circles*. The alanine at position 3 in the asparagine to alanine (N3A) analog is colored *red*. *B*, schematic representation of the various AgrC RHKs referred to in this study. The group I and group II chimeras have the polytopic sensor domains from the group I and group II receptors, respectively, fused to the group IV receptor HK domain.

AIP-I on activation by the AIP-II lactam was tested by inclusion of AIP-I at 100 nM or 1 μM during the assay. Cross-group inhibition experiments were performed using cell lines RN9222 (CA1-I) and RN9371 (CA4-IV), and self-inhibition experiments were performed using RN9372 (CA2-II) cells using agonists at a concentration of 100 nM.

Data Analysis—The data are plotted as initial β-lactamase reaction velocity *versus* log peptide concentration. In some instances, the data were normalized to percentage of maximal activation for curve-fitting purposes. Individual agonist concentration-response curves, in the absence and presence of antagonist, were fitted via nonlinear regression to the following four-parameter Hill equation, using PRISM 3.0 (Graph-Pad Software, San Diego, CA),

$$E = \text{basal} + \frac{E_{\max} - \text{basal}}{1 + 10^{(\log EC_{50} - \log [A])n_{\text{H}}}} \qquad \text{(Eq. 1)}$$

where E denotes effect, [A] is the agonist concentration, n_{H} is the midpoint slope, EC_{50} is the midpoint location parameter, and $E_{\max}$ and Basal are the upper and lower asymptotes, respectively.

Antagonist potency was subsequently determined by taking the agonist EC_{50} values obtained in the absence and presence of antagonist and fitting them to Equation 2 (21, 22) using nonlinear regression,

$$pEC_{50} = -\log([B]^s + 10^{-pK}) - \log c \qquad \text{(Eq. 2)}$$

where pEC_{50} is the negative logarithm of the EC_{50}, [B] is the antagonist concentration, pK and $\log c$ are fitting constants, and s is equivalent to the Schild slope factor. Curves were generated with either the Schild slope held constant at unity or allowed to vary, and the better-fitting model was determined by an extra sum of squares test using PRISM. In this test, a p value of <0.05 indicates a slope value significantly less than 1.

RESULTS

Identification of the Group Specificity Determinant of AgrC—AgrC consists of a divergent N-terminal sensor domain and a conserved C-terminal HK domain (5, 20), of which the former is predicted to contain the determinant of group specificity. To test this prediction, we constructed chimeric receptors (shown in Fig. 1*B*) in which the sensor domain of AgrC from either group I or II was fused to the HK domain of the group IV receptor (14). As shown in Fig. 2, the chimeric receptors were activated or inhibited only by AIP-I or AIP-II (from culture supernatants or chemically synthesized) according to their re-

spective sensor domains, thus confirming the above prediction. The group I chimera was activated not only by group I supernatant but also marginally by group IV supernatant, consistent with our previous results (14). Activation and inhibition titration curves of the chimeric receptors with synthetic AIP-I or AIP-II yielded curves similar to those previously reported for the wild-type group I and II receptors (18).

Activation by the Native AIP Is Reversible—Reversibility of agonist AIP binding to the receptor was analyzed by determining whether agonist activity could be reversed by washing or by competition from added antagonist. Since we have thus far not succeeded in developing a direct binding assay, functional assays of ligand binding and release were utilized, in which downstream reporter gene activation was used as a read-out of upstream ligand binding at the receptor (18). Such assays are highly sensitive due to downstream amplification of the binding event. In these experiments, group I cells were incubated with AIP-I at 1 μM, followed by washing as indicated in Fig. 3*A*. β-Lactamase activation was monitored, and the data were normalized at each time point. In the standard AIP assay without washing, the *agr* system was activated 25-fold during 180 min of incubation. Two washes decreased the activation to about 10-fold, and five and 10 washes variably decreased the activation further but never completely eliminated it. Competition experiments were conducted after two washes by adding AIP-II at 1 μM to resuspended cells. As can be seen in Fig. 3*A*, this completely abolished activation. An analogous experiment was performed with group II cells, where it was shown that 40-fold activation was reduced to 15-fold by two washes and was eliminated by the addition of AIP-I at 1 μM. Similar results were obtained when the truncated AIP-II (trAIP-II) was used as the antagonist of group II activation. In this case, 70-fold activation was reduced to 15-fold with two washes and abrogated completely by the addition of trAIP-II (Fig. 3*B*).

We have consistently observed a low level of β-lactamase activity in all of our experiments in the absence of added AIP. To test for the possibility that this might be *agr*-dependent, the
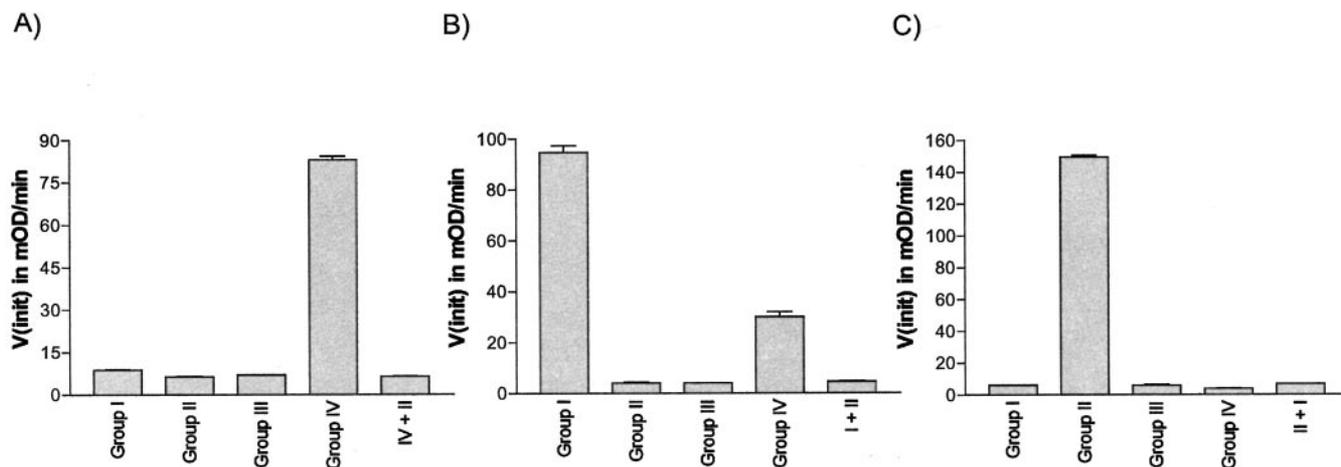
F1G. 2. **Chimeric receptor studies.** *A*, testing of the group IV receptor with bacterial supernatants from the four *agr* groups, collected as previously described (18). Cross-group inhibition was confirmed by co-incubating cells with AIP-II at 1 μM. *B*, testing of the group I chimera with bacterial supernatants from the four *agr* groups. Cross-group inhibition was demonstrated as in *A*. *C*, testing of the group II chimera with bacterial supernatants from the four *agr* groups. Cross-group inhibition was demonstrated by co-incubating cells with AIP-I at 1 μM. Data were collected as β-lactamase activity (V_{init} in mOD/min) and are shown $\pm$ S.E.

basal transcription level of the β-lactamase reporter gene was monitored in the presence or absence of antagonists. Group II cells were incubated for 1 h in the absence of agonist, followed by the addition of buffer and AIP-I or trAIP-II (both at 1 μM) and monitoring of β-lactamase activity and cell density over the next 3 h. Basal transcription proceeded at a constant rate per unit of cell mass, and this activity was not diminished in the presence of antagonists, demonstrating that this basal level is *agr*-independent.

Cross-group Inhibition of agr Signaling Is Reversible—There are a number of possible mechanisms for inhibition by the antagonist AIPs depending on whether or not the observed inhibition is reversible. If inhibition is reversible, pretreatment with antagonist should have no effect on subsequent activation. However, if inhibition is irreversible, pretreatment with antagonist followed by washout should prevent subsequent activation. This was tested by preincubation of group I cells with AIP-II, followed by washing and then challenge with AIP-I. Pretreatment with the antagonist *versus* buffer (followed by washing and then the addition of agonist) did not affect subsequent activation, since the induction ratios for pretreatment with buffer *versus* pretreatment with antagonist were 14.8 $\pm$ 2.7 and 13.9 $\pm$ 2.9, respectively. Thus, inhibition is reversible. Varying the time of preincubation from 5 min up to 1 h (or, in the case of activation, from 30 min to 1 h) gave results similar to those observed in the above experiment.

The kinetics of inhibition were analyzed by titration of AIP-II in the presence of AIP-I. In these experiments, the agonist was added to group I cells 5 min before, simultaneously, or 5 min after the antagonist, followed by a 1-h incubation period. Under the conditions used in this experiment, the three curves were indistinguishable within experimental error, with an IC$_{50}$ value of 281 $\pm$ 19 nM, and the maximal stimulation achieved was the same as that seen with activation by AIP-I alone.

Self-inhibition by trAIP-II Is Also Reversible—Since trAIP-II has the same ring structure as the native AIP, it is likely to bind to the same receptor site. Because this is the first AIP derivative showing self-inhibition, we wished to determine whether its antagonism was reversible, similar to that of the native cross-inhibitory AIPs. Accordingly, we tested trAIP-II for reversible self-inhibition, as performed for cross-inhibition above. Activation of group II cells by AIP-II over a 60-min incubation was unaffected by prior incubation with trAIP-II, yielding indistinguishable EC$_{50}$ values of 45 $\pm$ 5 nM. To probe

the mechanism of self-inhibition further, inhibition concentration-response curves were measured where AIP-II was added before, during, or after the global inhibitor. The three inhibition curves were indistinguishable within experimental error, with an IC$_{50}$ value for group II inhibition of 244 $\pm$ 12 nM.

Pharmacological Analysis of Concentration-Response Curves—Agonist concentration-response curves were generated with increasing concentrations of antagonist. Shown in Fig. 4*A* is an example of this type of experiment, in which AIP-I was used to activate group I cells in the presence of AIP-II at 0, 10, 100, and 1000 nM. In this example and in other experiments of this type, the agonist curves shifted in a parallel, dextral fashion with increasing concentrations of the antagonist, with no significant effect of the antagonist on the maximum response to the agonist. Other combinations giving qualitatively similar translocations of concentration response curves were group II cells with AIP-II in the presence of differing [AIP-I], group II cells with AIP-II in the presence of differing [trAIP-II], group I cells with AIP-I in the presence of differing [trAIP-II], and group I cells with AIP-I in the presence of differing [AIP-II lactam]. Since there is a reciprocal relationship between the AIPs in terms of activation and inhibition of their respective groups, we also performed the reciprocal experiment, namely antagonism by AIP-I of group II cells in the presence of differing [AIP-II]. Fig. 4*B* shows representative data from two experiments using a wide range of agonist concentrations. The data show that the inhibition curves also shift in a parallel, dextral fashion in the presence of increasing (maximally activating) concentrations of agonist.

The use of a wide range of antagonist concentrations in multiple experiments allowed for the assessment and quantification of the data according to a model of simple competitive antagonism (Equation 2), using nonlinear regression analysis (21, 22). The Schild slopes, *p* values, and pA$_2$ values obtained from these experiments are summarized in Table I. It is notable that in all cases tested, the slope values were considerably less than the value of unity normally seen with simple competitive antagonism.

Modification of One Residue in AIP-II Converts an Agonist to an Antagonist—Removal of the tail region of the group II AIP resulted in a self-inhibitory peptide; therefore, perhaps more subtle modification of the tail region would also produce self-antagonists. We originally observed that an AIP-II analog with
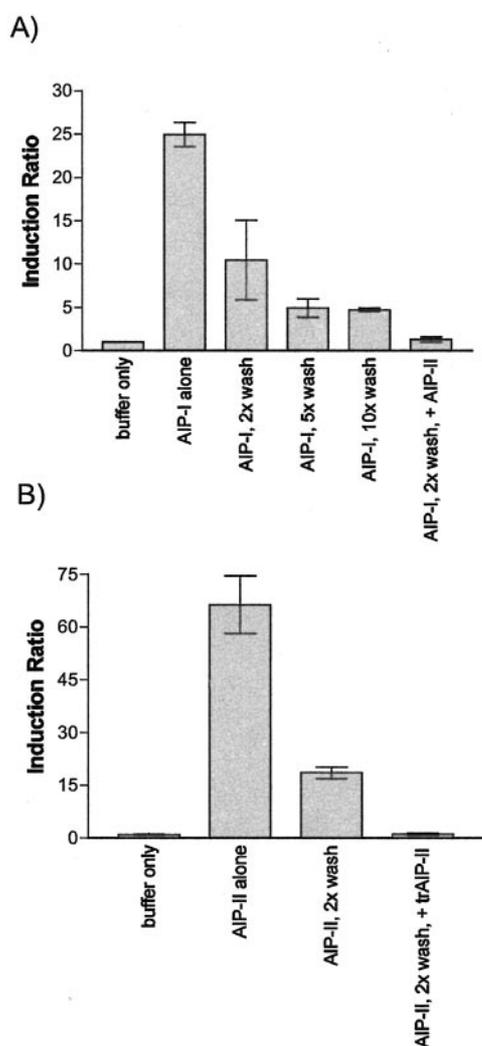
A)

B)

FIG. 3. **Functional binding and competition studies.** *A*, group I cells were activated with buffer or AIP-I at a concentration of 1 μM, followed by washes as indicated. For one set of cells, AIP-II was added after two washes at 1 μM. Data were collected as β-lactamase activity (V_{init} in mOD/min) and then normalized to an induction ratio (induced/basal). The data points from the final time point of activation (at 210 min) were combined from four separate experiments and are shown $\pm$ S.E. *B*, similar to *A*, except that group II cells were used with AIP-II as the agonist and trAIP-II as the antagonist.
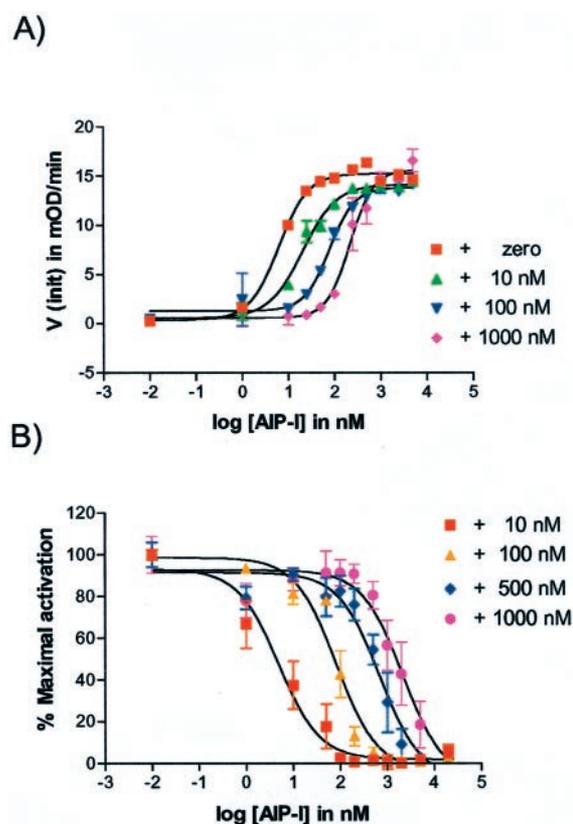
A)

B)

FIG. 4. **Pharmacological analysis.** *A*, group I cells were treated with varying [AIP-I] in the presence or absence of AIP-II at concentrations indicated as + *zero*, *10*, *100*, or *1000* nM. Data were collected as β-lactamase activity (V_{init} in mOD/min). Data are shown $\pm$ S.E. *B*, group II cells were treated with varying [AIP-I] in the presence or absence of AIP-II at concentrations indicated as + *10*, *100*, *500*, or *1000* nM.

TABLE I
Schild slope values

AIPs	Slope	*p* value	pA$_2$[a]
Group I inhibition[b]			
AIP-II	0.55 ± 0.14	0.016	8.90
AIP-II lactam	0.71 ± 0.09	0.012	7.60
trAIP-II	0.62 ± 0.05	0.130	6.50
Group II inhibition[b]			
AIP-I	0.45 ± 0.09	0.004	9.70
trAIP-II	0.55 ± 0.09	0.005	7.50

[a] The pA$_2$ is an estimate of antagonist potency, irrespective of underlying mechanism, determined via the relationship, pA$_2$ = pK/s (24).
[b] All experiments were performed at least in duplicate, yielding concentration-response curves in the presence of at least five different antagonist concentrations.

alanine in place of asparagine (N3A) in the tail region was a potent cross-inhibitor but was unable to self-activate and seemed also unable to self-inhibit (16). Using the more recently developed assay system in which no endogenous AIPs are produced (18), we now find that this peptide is, in fact, an antagonist of self-activation, with an IC$_{50}$ value of 180 ± 45 nM. This compares to an IC$_{50}$ value of 209 ± 39 nM for trAIP-II (18). These data suggest that a key molecular determinant of AIP-II-mediated receptor activation resides in the side chain of the asparagine residue. We have retested the other alanine-modified peptides synthesized previously and have confirmed the published results on those (16). This includes the lack of self-inhibition (up to 5 μM) by AIP-II analogs in which the remaining amino acids in the tail region and cyclic portion of the peptide were replaced by alanine.

The Lactam Analog of AIP-II Is an Agonist at High Concentrations—Williams and co-workers (23) have recently reported that the group I lactam analog is a self-activator at concentrations higher than 5 μM. We have now confirmed this result with AIP-II lactam, as shown in Fig. 5*A*. Starting at around 10 μM, activation increases linearly with increasing concentrations.

We also tested the lactam analog for its ability to cross-inhibit group I and group IV cells and to self-inhibit group II cells. We confirmed potent cross-inhibition, with an IC$_{50}$ value of 140 ± 70 nM for group I and 48 ± 22 nM for group IV but were unable to detect significant self-inhibition at any concentration tested up to 20 μM. These results suggest that the lactam analog binds to its own receptor extremely weakly, although it must bind heterologous receptors quite strongly.

The activation seen with the lactam analog was unusual in that we were unable to determine a maximal activation level, up to the solubility limit of the peptide (*i.e.* no plateau was observed). This is because the affinity of the lactam analog is so much lower (at least 1000-fold) than that of the native peptide. Thus, it was uncertain whether the activation by the lactam analog was truly specific to the receptor or a result of nonspecific effects of the peptide at such high concentrations. In order
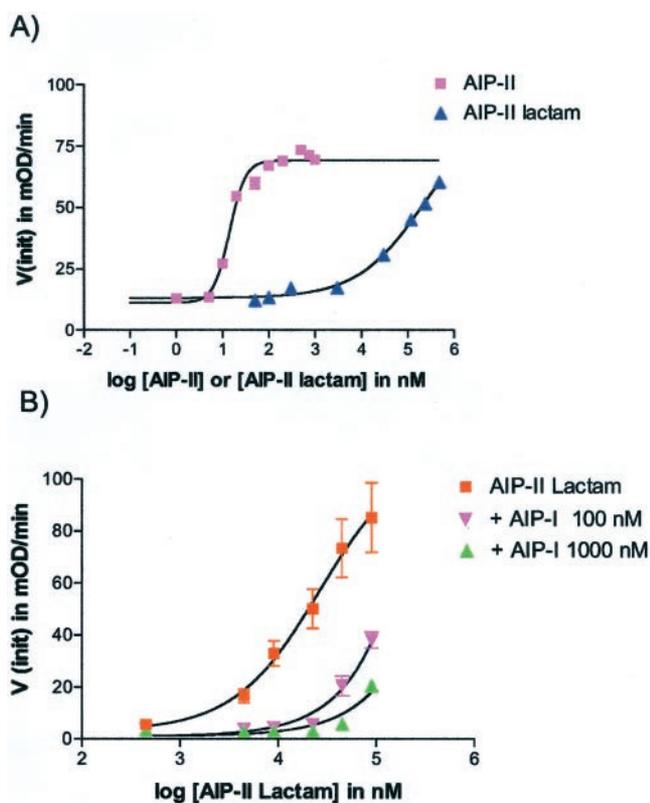
FIG. 5. **AIP lactam studies.** *A*, group II cells, RN9372 (CA2-II), were incubated with varying [AIP-II lactam]. The AIP-II concentration-response curve is shown for comparison. *B*, cells expressing group II *agrC-A* in an *agr*-null group I background, RN9367 (CA2-I), were incubated with the AIP-II lactam analog at various concentrations in the absence or presence of AIP-I at 0, 100, or 1000 nM. Data were collected as β-lactamase activity (V_{init} in mOD/min) and are shown ± S.E.

to address this specificity issue, two variables were investigated. First, if the activation were specific, it would be inhibited in a concentration-dependent manner by the antagonist, AIP-I. This is exactly what was observed, as shown in Fig. 5*B*. Second, it has been previously demonstrated that group-specific activation is independent of strain background (18). If the activation seen with the group II lactam is via the receptor, then this activation should also be strain-independent. This was indeed the case, as is shown in Fig. 5*B*, where activation of RN9367 (CA2-I) cells, similar to that seen with RN9372 (CA2-II) cells, was observed.

DISCUSSION

The *agr* signaling system in *S. aureus* is thus far unique in bacterial cell-cell signaling in that there are naturally occurring antagonists of the cell surface receptor, AgrC. The uniqueness of natural cross-inhibition by a bacterial autoinducer has prompted in depth studies of the *agr* ligand-receptor interaction and its inhibition. In the present study, our primary focus was on the reversibility (or irreversibility) of the *agr* AIP-receptor interaction. The theoretical basis for this focus was the possibility that the AIPs, with their highly reactive thiolactone bond, unique for signaling peptides, might act by acylating their receptor, leading to irreversible activation. This was supported by preliminary experiments in which it was not possible to eliminate AIP-induced signaling completely by extensive washing. However, a definitive test for reversibility was enabled by the natural antagonism among variant AIPs produced by strains belonging to different *agr* specificity groups. In these experiments, we used primarily the *agr* group I and II AIPs and their synthetic analogs *versus* test strains belonging to either group. Using several dif-

ferent experimental protocols, we have shown clearly that all of the AIP-receptor interactions that we have been able to test are completely reversed by an antagonist AIP. Thus, the residual activity remaining after extensive washing was eliminated by treatment of the cells with an antagonist, and only the relative concentrations of agonist and antagonist and not the order of their addition determined the outcome of an experiment. An extracellular site of action for the AIPs is supported by the chimeric receptor data (Fig. 2) as well as by the washout data (Fig. 3). Although these data and the results with the lactam analog rule out a stable covalent linkage between the AIPs and the receptor, we cannot formally rule out a transient covalent linkage formed between the AIP and receptor.

The lactam analogs of AIP-I (23) and AIP-II can activate their cognate receptors, but only at very high concentrations. Our finding that this activation is competitively blocked by a native heterologous AIP suggests that the lactam analog binds its cognate receptor on the same site as the native thiolactone, but only very weakly. Nonetheless, this does suggest that the highly reactive thiolactone linkage is not absolutely required for activation of the receptor. Furthermore, cross-inhibition by the AIP-II lactam analog is similar in potency to cross-inhibition by the native AIP-II, suggesting that the lactam binds the heterologous receptor with similar affinity as the native peptide. Thus, the cross-inhibitory action of the AIPs involves a binding interaction with the heterologous receptor that is very different from binding to the cognate receptor. The agonist and antagonist AIPs most likely bind in slightly different orientations to the same general region of the receptor such that the thioester group makes critical contacts with the receptor in one orientation (*i.e.* where the AIP and AgrC belong to the same group) but not in the other. This cross-inhibitory binding is also very permissive with respect to the AIP amino acid sequence, since many variant AIPs so far tested are strong antagonists although their sequences are highly divergent (13–15).

Pharmacological experiments were performed in which agonist concentration-response curves were measured in the presence of increasing concentrations of antagonist AIP. In all cases examined, the agonist and antagonist curves shifted in a parallel, dextral fashion with no depression of the agonist maximal response (Fig. 4, *A* and *B*). Qualitatively, these observations are consistent with a simple competitive interaction in which the agonist and antagonist AIPs compete for the same binding site on the receptor, AgrC. The data sets were also analyzed using the nonlinear regression method of Lew and Angus (21). As summarized in Table I, the calculated Schild slopes were all considerably less than unity. Surprisingly, this does not conform to a simple 1:1 competitive interaction, which predicts a Schild slope of 1. It should be noted, however, that because the assays in the current study quantified downstream transcriptional effects, mechanistic interpretations of the Schild slope factors and pA_2 values remain speculative until future (direct binding) experiments can determine such values more directly. This caveat aside, the results do raise the possibility that the receptor-ligand interaction occurs through some more subtle mechanism. In this regard, it is worth noting that bacterial RHKs are generally thought to be dimeric (3), raising at least the possibility of cooperativity between two AIP binding sites. Although this is an intriguing idea, additional experiments will be required to test this hypothesis.

The overall conclusions from these studies are (i) the N-terminal sensor domain of AgrC determines receptor specificity and contains the binding site for agonist and antagonist AIPs; (ii) AIPs bind a heterologous AgrC differently than the cognate receptor (the latter but not the former is profoundly affected by the substitution of a lactam for the native thiolactone); (iii)

certain modifications of the AIP generate a self-inhibitory peptide that is assumed to bind the same way as the native cognate AIP; (iv) agonist-antagonist interactions are reversible and probably competitive in that they involve overlapping binding sites; and (v) the key residue in the AIP-II tail region is the asparagine at position 4. Further structure-activity relationship studies of this position will illustrate the difference between self-activation and self-inhibition. In contrast, the endocyclic aspartate adjacent to the cysteine in AIP-I has been shown to be the key residue in terms of self-activation *versus* self-inhibition (23). This is consistent with the fact that AIP-I and AIP-IV differ only by one amino acid, an aspartate *versus* a tyrosine at this same position (14).

S. aureus is an important nosocomial pathogen that has developed resistance to most antibiotics and has lately become the focus of novel therapeutic initiatives. The data described herein have demonstrated that the mechanism of interference proceeds through reversible and specific extracellular antagonism of signaling through the sensor domain of AgrC. Given that there are many RHK-based systems in bacteria, plants, and other species, the design of molecules that compete with naturally occurring agonists for binding at RHK sensor domains could represent a generally applicable approach to the inhibition of RHK signaling.

REFERENCES

1. Sakakibara, H., Taniguchi, M., and Sugiyama, T. (2000) *Plant Mol. Biol.* **42,** 273–278
2. Groisman, E. A. (2001) *J. Bacteriol.* **183,** 1835–1842
3. Stock, A. M., Robinson, V. L., and Goudreau, P. N. (2000) *Annu. Rev. Biochem.* **69,** 183–215
4. Tomomori, C., Tanaka, T., Dutta, R., Park, H., Saha, S. K., Zhu, Y., Ishima, R., Liu, D., Tong, K. I., Kurokawa, H., Qian, H., Inouye, M., and Ikura, M. (1999) *Nat. Struct. Biol.* **6,** 729–734
5. Lina, G., Jarraud, S., Ji, G., Greenland, T., Pedraza, A., Etienne, J., Novick, R. P., and Vandenesch, F. (1998) *Mol. Microbiol.* **28,** 655–662
6. Havarstein, L. S., Gaustad, P., Nes, I. F., and Morrison, D. A. (1996) *Mol. Microbiol.* **21,** 863–869
7. Tortosa, P., and Dubnau, D. (1999) *Curr. Opin. Microbiol.* **2,** 588–592
8. Axelsson, L., and Holck, A. (1995) *J. Bacteriol.* **177,** 2125–2137
9. Wright, J. S., III, and Kadner, R. J. (2001) *J. Bacteriol.* **183,** 3149–3159
10. Novick, R. P., Ross, H. F., Projan, S. J., Kornblum, J., Kreiswirth, B., and Moghazeh, S. (1993) *EMBO J.* **12,** 3967–3975
11. Schauder, S., and Bassler, B. L. (2001) *Genes Dev.* **15,** 1468–1480
12. Winzer, K., and Williams, P. (2001) *Int. J. Med. Microbiol.* **291,** 131–143
13. Otto, M., Sussmuth, R., Jung, G., and Gotz, F. (1998) *FEBS Lett.* **424,** 89–94
14. Jarraud, S., Lyon, G. J., Figueiredo, A. M., Gerard, L., Vandenesch, F., Etienne, J., Muir, T. W., and Novick, R. P. (2000) *J. Bacteriol.* **182,** 6517–6522
15. Ji, G., Beavis, R., and Novick, R. P. (1997) *Science* **276,** 2027–2030
16. Mayville, P., Ji, G., Beavis, R., Yang, H., Goger, M., Novick, R. P., and Muir, T. W. (1999) *Proc. Natl. Acad. Sci. U. S. A.* **96,** 1218–1223
17. Otto, M., Sussmuth, R., Vuong, C., Jung, G., and Gotz, F. (1999) *FEBS Lett.* **450,** 257–262
18. Lyon, G. J., Mayville, P., Muir, T. W., and Novick, R. P. (2000) *Proc. Natl. Acad. Sci. U. S. A.* **97,** 13330–13335
19. Novick, R. P. (1991) *Methods Enzymol.* **204,** 587–636
20. Ji, G., Beavis, R. C., and Novick, R. P. (1995) *Proc. Natl. Acad. Sci. U. S. A.* **92,** 12055–12059
21. Lew, M. J., and Angus, J. A. (1995) *Trends Pharmacol. Sci.* **16,** 328–337
22. Christopoulos, A., Coles, P., Lay, L., Lew, M. J., and Angus, J. A. (2001) *Br. J. Pharmacol.* **132,** 1281–1291
23. McDowell, P., Affas, Z., Reynolds, C., Holden, M. T. G., Wood, S. J., Saint, S., Cockayne, A., Hill, P. J., Dodd, C. E. R., Bycroft, B. W., Chan, W. C., Williams, P. (2001) *Mol. Microbiol.* **41,** 503–512
24. Christopoulos, A., Parsons, A. M., and El-Fakahany, E. E. (1999) *J. Pharmacol. Exp. Ther.* **289,** 1220–1228